



Journal Name

COMMUNICATION

Phosphinecarboxamide as an unexpected phosphorus precursor in the chemical vapour deposition of zinc phosphide thin films

Received 00th January 20xx,
Accepted 00th January 20xx

Samuel V. F. Beddoe,^a Samuel D. Cosham,^a Alexander N. Kulak^b Andrew R. Jupp,^c Jose M. Goicoechea^c and Geoffrey Hyett^{a*}

DOI: 10.1039/x0xx00000x

www.rsc.org/

This paper demonstrates the use of phosphinecarboxamide as a facile phosphorus precursor, which can be used alongside zinc acetate for the chemical vapour deposition (CVD) of adherent and crystalline zinc phosphide films. Thin films of Zn₃P₂ have a number of potential applications and phosphinecarboxamide is a safer and more efficient precursor than the highly toxic, corrosive and flammable phosphine used in previous CVD syntheses.

Due to its high absorption coefficient ($> 10^4 \text{ cm}^{-1}$), direct band gap of 1.5 to 1.6 eV and long minority carrier diffusion length ($> 5 \mu\text{m}$), zinc phosphide is an excellent candidate for thin film photovoltaics.¹⁻⁵ Thin film photovoltaics have certain advantages over devices based on bulk semi-conductors; these include more efficient resource use and production of lighter weight devices which can be deposited onto a range of substrates, including flexible substrates. Zinc phosphide has a further advantage over other thin film photovoltaic candidate materials, such as cadmium telluride and $\text{CuIn}_x\text{Ga}_{(1-x)}\text{Se}_2$, due to its composition from Earth abundant elements. Zinc phosphide based devices have been developed with efficiencies of up to 6% using a Mg/p-Zn₃P₂ Schottky structure,⁶ and more recently combined with graphene to form a field effect solar cell.⁷ There is also a second area of interest for zinc phosphide in battery materials, as it has been shown to be a viable lithium anode material.⁸ However, both photovoltaic and battery applications require a route to a thin film of zinc phosphide.

Previous methods of thin film synthesis for zinc phosphide have included direct deposition, such as magnetron sputtering from either zinc phosphide crystals, or from zinc metal targets in the presence of phosphine gas.^{9, 10} Direct sublimation of high purity zinc phosphide powder can also be used to form films at low pressure using inert gas condensation.¹¹ Chemical vapour

deposition routes have also been used with potential advantages of increased adherence, non-line of sight deposition and more easily purified precursors - this final point a particular requirement of electronic grade materials. Previously reported CVD routes have made use of diethyl or dimethyl zinc as the zinc source, and phosphine as the phosphorus source.¹²⁻¹⁷ However, these precursors provide a number of challenges which make them undesirable for industrial and laboratory use. The zinc organometallic sources are pyrophoric, and phosphine is highly toxic, flammable and corrosive.

In this paper we identify zinc acetate and phosphinecarboxamide ($\text{PH}_2\text{C}(\text{O})\text{NH}_2$) as a precursor combination which can be used with aerosol assisted chemical vapour deposition (AACVD), a variant in which the precursors are transported to the reactor *via* an aerosol mist, rather than as a vapour.¹⁸⁻²⁰ AACVD allows a much wider range of potential precursors to be investigated, with the limiting factor being the solubility of the precursor compound in the chosen solvent rather than its volatility. Both phosphinecarboxamide and zinc acetate are soluble in methanol, and can be used to rapidly form adherent and crystalline films of zinc phosphide using AACVD. Zinc acetate is indefinitely stable in air, while $\text{PH}_2\text{C}(\text{O})\text{NH}_2$ is air and moisture stable for several days in solution, although it was kept as a solid in an inert atmosphere glove box for long term storage. As such, these precursors provide a CVD route to zinc phosphide films for electronic applications without the pyrophoric and toxicity concerns of previously used precursors.

The zinc phosphide films were deposited by AACVD on float glass substrates (25 x 150 x 4 mm³ Pilkington NSG) using a hot-wall reactor which has been described in detail previously,²¹ but in summary is a quartz tube with a graphite block substrate support, held in a tube furnace as the heat source. The precursor solution was held in a 100 ml three-necked round bottom flask, partially immersed in water with a piezoelectric humidifier (Maplin, L38AK) used to generate the aerosol mist. Zinc(II) acetate (Sigma Aldrich 99.99%) and methanol (Fisher Scientific, technical grade) were purchased and used as supplied. Phosphinecarboxamide was synthesized as previously reported from the reaction of sodium phosphoethynolate with ammonium chloride.²² Each experiment

^a Department of Chemistry, University of Southampton, Southampton, SO17 1BJ, UK

^b School of Chemistry, University of Leeds, Leeds, LS2 9JT, UK

^c Department of Chemistry, Chemistry Research Laboratory, University of Oxford, Mansfield Road, Oxford, OX1 3TA, UK

* Corresponding author. Please contact at g.hyett@soton.ac.uk
Electronic Supplementary Information (ESI) available: [details of any supplementary information available should be included here]. See DOI: 10.1039/x0xx00000x

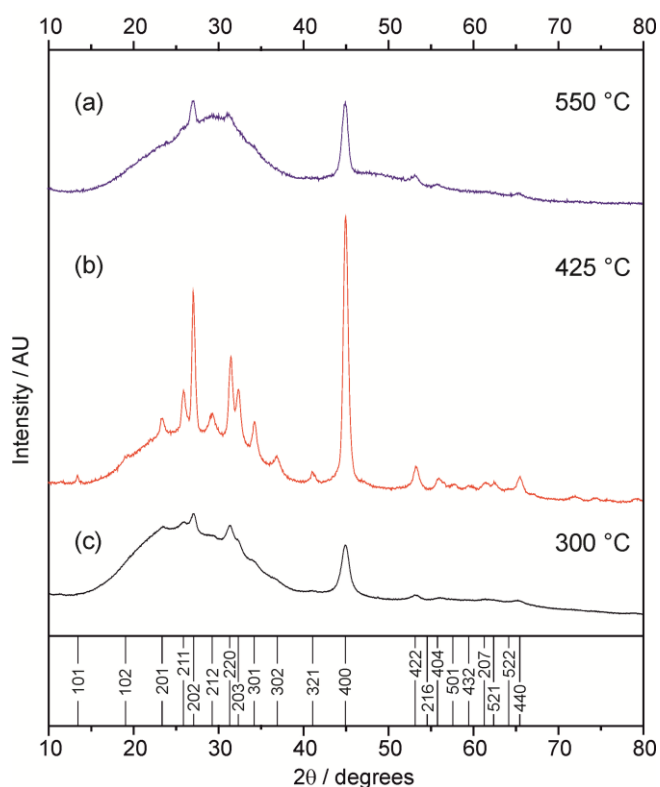


Figure 1. X-ray diffraction patterns collected from zinc phosphide films synthesized from zinc acetate and phosphinecarboxamide at: (a) 550 °C (b) 425 °C and (c) 300 °C. Inset below the patterns shows the expected Bragg reflections with hkl labels for zinc phosphide (Zn_3P_2) crystallising in $P4_2/nmc$ with $a = 8.0905$ Å and $c = 11.414$ Å, taken from the ICSD 603896. Note that for clarity only the most intense peaks are shown, up to 65° two theta.

used equal molar quantities of phosphinecarboxamide and zinc acetate (8.4×10^{-4} moles) in 25 ml of methanol, with the aerosol transported to the reactor under a flow of argon gas (BOC, 0.5 L min^{-1}). Reactions were carried out at substrate temperatures of 300 °C, 425 °C and 550 °C, and took 40 to 50 mins to reach completion. The films were analysed using grazing incident X-ray diffraction, UV-vis-NIR spectroscopy and scanning electron microscopy.

Depositions using zinc acetate and phosphinecarboxamide were successful at all three temperatures, from 300 °C to 550 °C, with X-ray diffraction measurements confirming that tetragonal Zn_3P_2 had been deposited in each case (Figure 1). For the diffraction data collected from these films, Rietveld refinements were able to provide a good match to the expected peak intensity for Zn_3P_2 indicating little preferred orientation, with lattice parameters slightly smaller than those reported in the literature. Rietveld fits can be found in the ESI. For our films the a lattice parameter was found in the range 8.04 to 8.07 Å with c in the range 11.32 to 11.41 Å, compared to previously reported bulk values of $a = 8.09$ Å and $c = 11.41$ Å.²³ Peak broadening is also observed in the diffraction data, and Scherrer analysis can be used to estimate the crystallite size.²⁴ For the three samples this gives crystallite sizes of 80 nm, 130 nm and 105 nm for the films deposited at 300, 425 and 550 °C respectively. No additional Bragg peaks could be identified in the diffraction data, and crucially no peaks attributable to contaminants arising from oxidation or hydrolysis of the zinc phosphide films, such as ZnO , $Zn(OH)_2$, or $Zn_3(PO_4)_2$ were observed despite prolonged storage of samples in air, and use of methanol and the

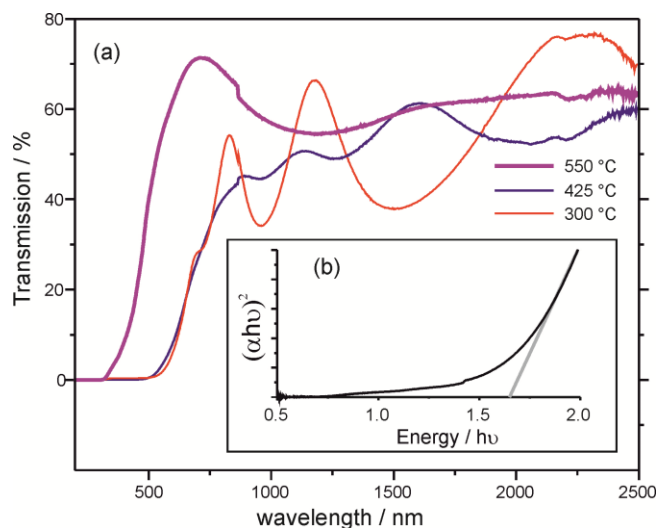


Figure 2. (a) Transmission spectra recorded on the zinc phosphide films deposited onto float glass, deposited at three different temperatures. (b) Inset shows an example Tauc plot for the film deposited at 300 °C.

acetate salt of zinc, both of which could be possible sources of oxygen within the deposition.

Transmission spectra were recorded across the UV to near IR range of 200 to 2500 nm for all three films, and these are shown in Figure 2(a). The method described by Swanpoel allows estimation of the film thickness from observed interference in the transmission spectra, if a sufficient number of fringes can be observed.²⁵ For the films synthesized at 300 °C and 425 °C this approach gives thickness values of 380 nm and 1174 nm. The film synthesised at the highest temperature, 550 °C, is too thin to apply this method, as an insufficient number of interference fringes can be observed in the spectral range recorded. Modelling of the transmission spectra using expressions derived by Nilsson,²⁶ with previously reported literature values of the refractive index of zinc phosphide,¹ indicate that the film must be approximately 120 nm in thickness in order for only a single interference fringe to be observed at a wavelength of 1200 nm, as seen in Figure 2. The significantly greater film thickness observed for the film deposited at 425 °C helps to account for the greater X-ray diffraction pattern intensity observed for this film in Figure 1, compared to the data collected on the films deposited at higher and lower temperatures. The spectra can also be used to estimate the band gap of each material, using the Tauc method.²⁷ This provides values of 1.59 to 1.65 eV, depending on temperature of deposition as reported in Table 1. These are similar to but slightly larger than the previously reported value of 1.6 eV for bulk zinc phosphide;¹ this increase from the bulk might be due to the stress or reduced crystallite size observed from the XRD data. However it should be noted that the exact value of the band gap remains a matter of controversy, and is dependent on the methodology used to determine it.⁵

Dep. Temp/ °C	Thickness / nm	Crystallite Size / nm	Lattice Parameters		Band Gap/ eV	P/Zn Ratio
			a / Å	c / Å		
300 °C	380	80	8.079(1)	11.376(1)	1.65	0.62
425 °C	1174	130	8.044(1)	11.425(1)	1.59	0.82
550 °C	~120	105	8.073(1)	11.319(1)	1.62	0.48

Table 1. Summary of analysis of the zinc phosphide films deposited at temperatures from 300 °C to 550 °C. Data shown are thickness determined from transmission data, lattice parameters and crystallite size from XRD, band gap from Tauc plots and P/Zn ratio from EDX analysis.

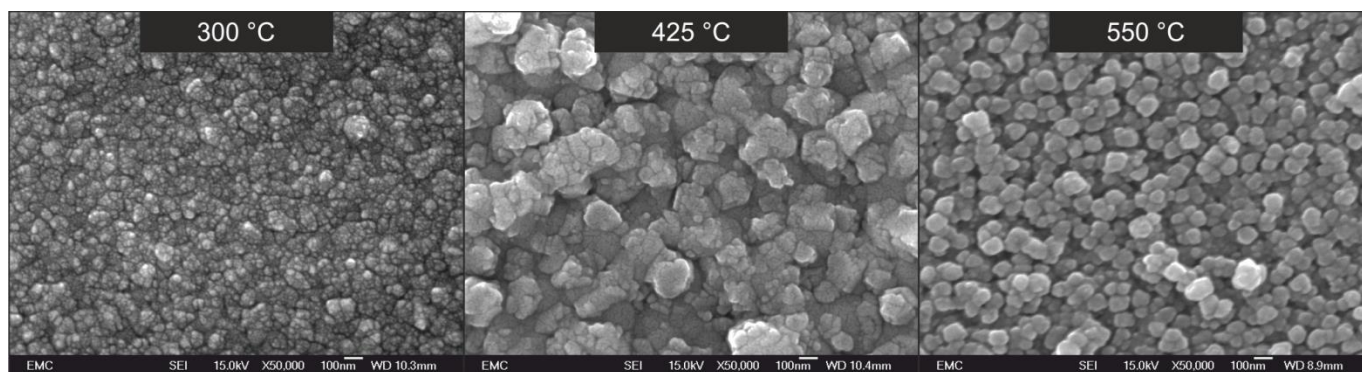


Figure 3. SEM images of the three zinc phosphide films deposited at different temperatures.

Elemental composition of the films was determined using EDX, collected using an accelerating voltage of 10 keV, with three spots investigated on each film and averaged to provide the composition. In all films both zinc and phosphorus could be detected, confirming the composition, alongside peaks assigned to O, Si, Al, Na, and Mg. These latter elements are associated with the glass substrate, observed due to overshoot of the electron beam through the film. EDX confirms qualitatively the expected elemental composition; however, quantitative analysis is hindered due to differing element absorption lengths combined with the variation in sample thickness, surface roughness and overshoot. The phosphorus to zinc ratios reported in Table 1 from 0.48 to 0.82 are consistent within each sample across the three sampled sites, but show clear variation due to the above mentioned factors, and so in this case EDX cannot be used for reliable quantitative analysis.

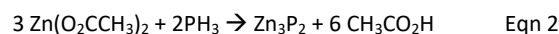
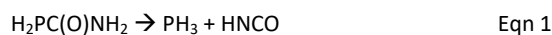
SEM images of the films are shown in Figure 3. These show a relatively smooth film for the sample grown at 300 °C, with small particle size of 50 to 100 nm. At higher temperatures, larger particles, around 100 nm to 200 nm, and rougher surfaces are observed. No distinct anisotropy, crystal morphology or orientation can be discerned from the images. These results correlate well with the absence of preferred orientation observed in the diffraction patterns, and also with the crystallite size distributions determined from Scherrer analysis. Additional side-on SEM images and EDX mapping measurements were carried out, and these can be found in the ESI Figure S3. The EDX mapping shows a distinct segregation between the zinc and phosphorus signals from the film, and oxygen signals on the substrate, confirming that oxygen contamination in the bulk of the film is minimal.

The XRD and spectral data confirm that films of zinc phosphide can be successfully made from zinc acetate and phosphinecarboxamide, across a range of temperatures from 300 °C to 550 °C, and that these films are adherent and crystalline. For this precursor combination the optimal growth temperature for the conditions tested is 425 °C, with this providing the largest crystallite size and greatest film thickness, with a growth rate of 26 nm min⁻¹. Previous methods of CVD zinc phosphide film formation from alkyl zinc and phosphine has been successful from 225 °C to 550 °C, however some reports have required an initial high temperature 800 °C phosphine cracking step to activate the phosphorus source.¹² These have also shown slower growth rates of 1 to 10 nm min⁻¹. These previous CVD routes also require an excess of phosphine, typically

reported with a phosphorus to zinc source ratio of 6:1, compared to our more atom efficient 1:1 ratio.^{12, 14} In terms of growth rate and crystallinity the use of AACVD with zinc acetate and phosphinecarboxamide produces films equal or superior in quality to those grown with MOCVD from phosphine and dimethyl zinc.

Zinc acetate is a well-established zinc source in AACVD, and in fact may be used as a single source precursor to zinc oxide.²⁸ However, despite its ability to deliver both zinc and oxygen it has also been shown to be able to form non-oxide films when used with an appropriate co-reagent, for example with the formation of zinc carbodiimide and zinc sulphide through the addition of urea and thiourea respectively to the precursor solutions.^{29, 30} The key novelty of this work, then, is the demonstration of phosphinecarboxamide as a source of phosphorus that can be used in conjunction with zinc acetate.

Some understanding of the mechanism of zinc phosphide formation in this system can be derived from solution NMR studies. ³¹P and ³¹P{¹H} NMR were carried out using a 400 MHz spectrometer on a solution of zinc acetate and phosphinecarboxamide. This showed a single phosphorus resonance at -136.9 ppm in the decoupled spectra, and a triplet of doublets in the ³¹P NMR spectra (Figure S4, ¹J_{P-H} = 210 Hz, 3J_{P-H} = 12 Hz), consistent with previously reported spectra on free phosphinecarboxamide alone.²² Additionally, when co-ordination to a metal centre was reported in W(CO)₅[PH₂C(O)NH₂] a shift of 34.9 ppm was observed, alongside significant changes to the coupling pattern.³¹ Therefore NMR evidence suggests that zinc acetate and phosphinecarboxamide are stable together in solution, and that no intermediate precursor complex is formed.



However, previous studies have shown that prolonged heating above 75 °C does lead to the decomposition of phosphinecarboxamide into phosphine and isocyanic acid (Eqn 1),²² and this will almost certainly occur under the much higher temperatures found in the reactor. The most likely scenario is that this *in situ* generated phosphine can then react with the zinc acetate either in the gas phase or at the substrate and form the desired zinc phosphide film (Eqn 2), as experiments with exposure of pre-made zinc oxide films did not lead to any conversion to zinc

phosphide. In both cases the methanol solvent is assumed to be an inert carrier, although urea methanolysis is known, and may aid in the decomposition of $\text{PH}_2\text{C}(\text{O})\text{NH}_2$ under the reaction conditions.³²

Conclusions

In this paper we provide a new route to the formation of zinc phosphide thin films using zinc acetate and phosphinecarboxamide by aerosol assisted chemical vapour deposition. The films deposited are crystalline and adherent, and these two precursors represent a significant improvement in atom efficiency, ease of handling and safety compared to previously described CVD routes. This work also highlights the possibility of making use of phosphinecarboxamide as a general source of phosphorus in chemical vapour deposition.

Conflicts of interest

There are no conflicts to declare.

Notes and references

- 1 E. A. Fagen, *J. Appl. Phys.*, 1979, **50**, 6505
- 2 C. Wadia, A. P. Alivisatos and D. M. Kammen, *Environmental Science & Technology*, 2009, **43**, 2072
- 3 J. Collier, S. Wu and D. Apul, *Energy*, 2014, **74**, 314
- 4 N. C. Wyeth and A. Catalano, *J. Appl. Phys.*, 1979, **50**, 1403
- 5 G. M. Kimball, A. M. Müller, N. S. Lewis and H. A. Atwater, *Appl. Phys. Lett.*, 2009, **95**, 112103.
- 6 M. Bhushan and A. Catalano, *Appl. Phys. Lett.*, 1981, **38**, 39
- 7 O. Vazquez-Mena, J. P. Bosco, O. Ergen, H. I. Rasool, A. Fathalizadeh, M. Tosun, M. Crommie, A. Javey, H. A. Atwater and A. Zettl, *Nano Lett.*, 2014, **14**, 4280
- 8 W. W. Li, L. Gan, K. Guo, L. B. Ke, Y. Q. Wei, H. Q. Li, G. Z. Shen and T. Y. Zhai, *Nanoscale*, 2016, **8**, 8666
- 9 A. Weber, P. Sutter and H. von Känel, *Thin Solid Films*, 1994, **239**, 205
- 10 M. Sharma, M. Mushrush, R. J. Wright, N. Shinkel, S. Sprague, S. Rozeveld, M. Woodward, K. Kearns, P. Small and C. Todd, *Thin Solid Films*, 2015, **591**, 32.
- 11 I. K. El Zawawi, A. Abdel Moez, T. R. Hammad and R. S. Ibrahim, *Superlattices Microstruct.*, 2014, **75**, 183
- 12 A. M. Hermann, A. Madan, M. W. Wanlass, V. Badri, R. Ahrenkiel, S. Morrison and C. Gonzalez, *Sol. Energy Mater. Sol. Cells*, 2004, **82**, 241
- 13 K. Kakishita, T. Baba and T. Suda, *Thin Solid Films*, 1998, **334**, 25
- 14 T. L. Chu, S. S. Chu, K. Murthy, E. D. Stokes and P. E. Russell, *J. Appl. Phys.*, 1983, **54**, 2063.
- 15 J. Long, *J. Electrochem. Soc.*, 1983, **130**, 725
- 16 E. Papazoglou and T. W. F. Russell, *Journal of Vacuum Science & Technology a-Vacuum Surfaces and Films*, 1987, **5**, 3378
- 17 Y. Kato, S. Kurita and T. Suda, *J. Appl. Phys.*, 1987, **62**, 3733
- 18 P. Marchand, I. A. Hassan, I. P. Parkin and C. J. Carmalt, *Dalton Trans.*, 2013, **42**, 9406
- 19 M. J. Powell and C. J. Carmalt, *Chemistry – A European Journal*, 2017, **23**, 15543.
- 20 C. E. Knapp and C. J. Carmalt, *Chem. Soc. Rev.*, 2016, **45**, 1036
- 21 N. J. Platt, K. M. Kaye, G. J. Limburn, S. D. Cosham, A. N. Kulak, R. G. Palgrave and G. Hyett, *Dalton Trans.*, 2017, **46**, 1975.
- 22 A. R. Jupp and J. M. Goicoechea, *J. Am. Chem. Soc.*, 2013, **135**, 19131
- 23 U. Elrod, M. Luxsteiner, E. Bucher, J. Honigschmid, K. Bickmann and L. Gain, *J. Cryst. Growth*, 1984, **67**, 195
- 24 A. L. Patterson, *Physical Review*, 1939, **56**, 978
- 25 R. Swanepoel, *Journal of Physics E-Scientific Instruments*, 1983, **16**, 1214
- 26 P. O. Nilsson, *Appl. Opt.*, 1968, **7**, 435
- 27 J. Tauc, *Mater. Res. Bull.*, 1968, **3**, 37
- 28 M. R. Waugh, G. Hyett and I. P. Parkin, *Chem. Vap. Deposition*, 2008, **14**, 366
- 29 K. M. Kaye, W. Grantham and G. Hyett, *Chem. Vap. Deposition*, 2015, **21**, 281
- 30 M. A. Hernandez-Fenollosa, M. C. Lopez, V. Donderis, M. Gonzalez, B. Mari and J. R. Ramos-Barrado, *Thin Solid Films*, 2008, **516**, 1622
- 31 M. B. Geeson, A. R. Jupp, J. E. McGrady and J. M. Goicoechea, *Chem. Comm.*, 2014, **50**, 12281
- 32 H. Wang, M. H. Wang, W. B. Zhao, W. Wei and Y. A. Sun, *Reaction Kinetics Mechanisms and Catalysis*, 2010, **99**, 381